Eurasian J. Sci. Eng., 2025, 11(2), 179-195
https://doi.org/10.23918/eajse.v11i2p12

Published by Tishk International University
Available at: https://eajse.tiu.edu.iq/

RESEARCH ARTICLE Open Access

Radiation Protection Properties of Binary and Tertiary Tellurite Glasses: Comparative Study

Didar Swara Salih[1] *, Shaida Anwer kakil [2], and Mohammed Issa Hussein[2]

[1] Department of Physiotherapy, Erbil Technical Health College, Erbil Polytechnic University, Erbil, Kurdistan -Region, Iraq

[2] Department of Physics, College of Science, Salahaddin University-Erbil, Erbil Kurdistan Region, Iraq.

Article History
Received: 09.03.2025
Revised: 01.08.2025
Accepted: 14.08.2025
Published: 19.08.2025
Communicated by: Prof. Dr. Suhairul Hashim
*Email address:
didar.salih@epu.edu.iq
*Corresponding Author

Abstract: The theoretical estimation of the radiation shielding property was done for a series of binary and ternary tellurite glasses. TeO_2-based glasses were modified with some binary chemicals like Bi_2O_3, WO_3, ZnO, and PbO, along with their ternary combinations including Ta_2O_5. Their mass attenuation coefficient, effective atomic number, and electron density have been computed to study the efficiency of such glasses in gamma-ray shielding. It has been found that the binary composition of TeO_2 + Bi_2O_3 has greater shielding efficiency than other binary glasses. Among the ternary combinations, the TeO_2 + Bi_2O_3 + PbO glass was confirmed as the most efficient material. This work testifies to the efficiency of the tellurite glasses for their use as promising materials in radiation shielding applications due to the improved performance with the addition of Bi_2O_3 and PbO. A comparative analysis is performed to determine which glass compositions offer the most efficient radiation attenuation. The results aim to guide the design of advanced radiation shielding materials for medical, nuclear, and industrial applications.

Keywords: *TeO2; Binary; And Ternary; Half And Tenth Value Layer; Effective Atomic Number; And Electron Density State*

1. Introduction

The study of metal oxide-modified tellurite glass systems for radiation shielding presents a fascinating crossroads of materials science and nuclear engineering. Basically, tellurite glasses are TeO2 with other added oxides that have been studied for their unique properties: high refractive index,[1,2]good thermal stability, [3] and excellent optical transmission in the infrared region. [4-6]These features make them attractive hosts for different applications, including telecommunications, photonics, and sensing.[1] The addition of metal oxides to tellurite glass matrices can add to their potential use in radiation shielding.[8] There are metal oxides that have high atomic numbers; examples include PbO, Bi2O3, and WO3,[3] which can interact effectively with ionizing radiation and hence reduce its penetration in a material.[4]–[7] Most probably, the work will be focused on the detailed study of composition-property relationships of the modified tellurite glass systems. ZnO, in combination with other materials, can be used for radiation shielding, especially in medical and industrial settings. It's been used in nanocomposite forms to provide protection from various forms of radiation, including X-rays and gamma rays.[14,15]

The growing use of radiation in fields like medical imaging, nuclear power generation, and industry has raised the demand for efficient materials for shielding against radiation. Tellurite glasses have emerged as potential candidates because of their structural features, high density, and transparency to visible light. Among these, binary and ternary tellurite glasses are of particular interest for their

potential to provide enhanced radiation shielding. [12,16] In summary, research into tellurite glass systems enhanced with metal oxides offers significant potential for advancing the development of high-performance materials designed to attenuate the detrimental effects of ionizing radiation. Such materials hold considerable promise for diverse applications, including industrial, medical, and nuclear sectors, where effective radiation shielding is critical. [12,13,17-19] Prior research has demonstrated the attenuation characteristics of TeO_2-based glasses, including diverse metal oxides, both theoretically and empirically. M.S. Al-Buriahi et al. have explored the influence of TeO_2 on modifying the radiation shielding capacity of calcium boro-tellurite glasses. Aljawhara H. Almuqrin et al. have established the efficacy of the Phy-X program in quantitatively evaluating the radiation shielding capacity of glasses and materials. Ravangvong et al. have explored the influence of WO_3 on the radiation shielding efficiency of the binary tellurite glass system of composition WO_3–TeO_2. Tijani S.A. et al. have explored the influence of TeO_2 and Bi_2O_3 on the efficacy of the radiation shielding of lead-free transparent bismuth tellurite glasses with special focus on the region of low gamma energy. Al-Hadeethi and Sayyed have applied the Phy-X software for the analysis of the influence of the variation of the content of BaO from 40 to 50 mol% on the radiation shielding capacity of CaF_2-BaO-P_2O_5 glasses. Sayyed et al. have also explored the influence of ZnO in the TeO_2-ZnO-Fe_2O_3 glass matrix on the radiation shielding characteristics of the latter using Phy-X software for energy levels of 0.284 to 2.506 MeV. They have also compared the attenuation of their glass system with that of other glasses at 0.662 MeV.

The radiation shielding properties were theoretically investigated using the Phy-X software, a computational tool renowned for its accuracy in analyzing material performance against radiation.

In this study focuses on the comparative evaluation of radiation shielding properties in binary tellurite glass samples in the form TeO_2 + ZnO, TeO_2 + WO_3, TeO_2 + Bi_2O_3, TeO_2 + PbO and ternary tellurite glass samples in the form TeO_2 + ZnO + WO_3, TeO_2 + ZnO + Ta_2O_5, TeO_2 + WO_3 + Bi_2O_3, TeO_2 + Bi_2O_3 + PbO, and TeO_2 + PbO + ZnO, Notably, critical parameters such as the mass attenuation coefficient ($\mu\rho$), effective atomic number (Z_{eff}), effective electron density (N_{eff}), half-value layer (HVL), tenth-value layer (TVL), and mean free path (MFP) have been calculated and compared to examine the efficacy of such materials for attenuation of various types of radiation. By systematic comparison of the parameters, this work aims to identify the most effective glass composition with optimal shielding performance. Results are likely to yield valuable information for the design and fabrication of new materials for the purpose of radiation shielding.

Furthermore, computational modelling and simulation techniques may complement experimental efforts, providing insights into the essential processes regulating radiation interaction inside the glass matrix. This interdisciplinary approach enables the optimization of glass composition to achieve the desired balance between radiation shielding effectiveness, mechanical properties, and other relevant factors.[20,21]

2. Materials and methods

The determination of photon attenuation properties of materials is of crucial relevance in designing new advanced shielding solutions for radiation. Manually computing photon attenuation parameters with precision is inherently cumbersome and time-consuming when selecting and classifying materials for shielding applications in various areas of technology. It is hence critical to compute such parameters rapidly, conveniently, and with precision either across the continuous energy range or at specific energy points to select the most suitable material from a set when designing new shielding systems. In this research work, we employed the simple-to-use web-based Photon Shielding and Dosimetry (Phy-X/PSD) program [21] to compute shielding- and dosimetry-related quantities. With this program, one can compute eighteen photon attenuation parameters at any selected energy point within minutes. It is

enough for users to provide the chemical composition of the material, density, and energy values, upon which the program outputs the corresponding photon attenuation values. Out of the eighteen computed parameters, the most crucial for the determination of the photon attenuation ability of any material is the mass attenuation coefficient (μ_ρ) because it quantitatively characterizes the photon-material atomic structure interaction. Additionally, μρ is also the basis for the computation of other quantities such as electron density N_{eff}, linear attenuation coefficient μ, and effective atomic number Z_{eff}, among many others.[22]

Gamma rays of certain energies are attenuated in matter through three primary mechanisms of interactions: the photoelectric effect, Compton scattering, and pair production. The intensity of the radiation falls off exponentially as it passes through the thickness of the absorbing material quantitatively described by the equation of exponential attenuation.:

(1) $$I = Ie^{-\mu x}$$

Here, I0 and I are the incident and transmitted γ-ray intensities, respectively, xx is the absorbing medium thickness, and μ is the linear attenuation coefficient with units of cm−1. Linear attenuation coefficient μ is one of the most critical shielding parameters and is a function of γ-ray energy and absorbing material composition.

The other shield parameters, such as half-value layer (HVL) and tenth-value layer (TVL), were also calculated using Eqs. (2) and (3). They are the absorber thicknesses required to reduce the γ-ray intensity to 50% and 10% of their initial values, respectively.[23,27, 29–45]:

(2) $$HVL = \frac{Ln\ 2}{\mu}$$

(3) $$TVL = \frac{Ln\ 10}{\mu}$$

Furthermore, the effective atomic number of relevance for gamma-ray interactions in compounds and composites as opposed to pure elements was computed using Eq. (4). [30–32]:

(4) $$Z_{eff} = \frac{\sum_i f_i A_i \mu_i}{\sum_j f_j \frac{A_j}{Z_j} \mu_j}$$

Here, Ai, Zi, and fifi are the atomic weight, atomic number of the ith component element of the material composition, and molar fraction, respectively.

The effective electron density (N_{eff}) is calculated using Eq. (5) as the number of electrons per unit mass of the composite material. [33-38]:

(5) $$N_{eff} = N_A \frac{Z_{eff}}{\langle A \rangle}$$

NA is Avogadro's number and ⟨A⟩ = ∑ifiAi⟨A⟩ is the mean atomic mass of the composite material.

3. Result and Discussion

3.1 Mass coefficient attenuation

The mass attenuation coefficient (μ/ρ) is the measure of the extent to which a material reduces the intensity of a beam of radiation for each unit of mass. It varies with the energy of the incident photons and with the atomic structure of the material. It is crucial for applications in the fields of material characterization and radiation shielding.

The investigation of the mass attenuation coefficient is presented for two panels, each focused on different TeO_2 (Tellurium dioxide) mixes. The detailed discussion on the mass attenuation coefficient for TeO_2-based binary mixture samples is shown in Fig.1 and Panel (a). This panel reveals variation in the attenuation coefficient with photon energy range for these two-component systems, which provides a clear idea of the role of TeO_2 in the modification of photon interaction inside binary mixtures. Results showed large variation, especially by the mixture composition as well as by the photon energy range of 0.1-100 MeV.

The attenuation coefficient generally diminishes as photon energy increases, due to high-energy photons give rise to less opportunity of being interacted with or taken off by the material. Overall energy variance, the variation in a mass attenuation coefficient in energy for a binaryTeO_2 -ZnO combination in its pictorial representation would lie across the fluctuations. Specific changes happen, which are decided by the interaction characteristics of ZnO and TeO_2. In the combination of TeO_2 + WO_3, a similar trend is observed, where the attenuation coefficient diminishes as photon energy increases. WO_3 provides additional attenuation features due to its special interaction features with photons, leading to abnormal fluctuation features. High-Z materials like Bi_2O_3 and PbO mixed with TeO_2, on the other hand, show high variations in attenuation, especially at lower energies of photons. In these combinations, TeO_2 + Bi_2O_3, TeO_2+ Pb, the mass attenuation coefficient generally diminishes as photon energy increases, [39] Panel (b) presents the oscillations of the mass attenuation coefficient for the ternary mixtures containing TeO_2. This panel addresses the behavior of three-component systems and focuses on the contribution of TeO_2 to the photon attenuation in these complex mixes. The mixture of TeO_2, ZnO, and WO_3 shows a complex oscillation due to the synergistic interaction of ZnO and WO_3. The variation at different energies of photons shows the complication of these components interacting with each other to give that fine response due to the photons. Inclusions of Ta_2O_5 within a mixture of TeO_2+ZnO result in the incorporation of new attenuating properties.

The mass attenuation coefficient varies within the range of the binary mixtures, especially at particular photon energies. These variations are ascribed to some unique features of Ta_2O_5, which change the course of attenuation. TeO_2 + WO_3 + Bi_2O_3 and TeO_2 + Bi_2O_3 + PbO mixtures represent high photon absorption values at low energies, primarily because of the incorporation of high-atomic-number elements, namely W, Bi, and Pb. [39-41], which elements contribute to a higher X-ray interaction with the proposed mixes. The attenuation profile of the binary TeO_2-PbO-ZnO is, by nature, intricate. As the variation of the mass attenuation coefficient has an impact on the overall attenuation, the TeO_2-PbO glass combines both PbO and ZnO in its composition with TeO_2 in such a way that a complex pattern of their interaction with photons over an energy spectrum comes into play.

The study indicates that the mass attenuation coefficient for TeO_2 blends is highly sensitive to the composition of the mixtures and to the photon. The TeO_2-based glasses contain various metal oxides to attenuate X-ray photon energy effectively. All the binary and ternary chemical combinations have different attenuation properties. In particular, the binary mixtures such as TeO_2 + Bi_2O_3 and ternary mixtures such as TeO_2 + Bi_2O_3 + PbO normally show a decrease in the mass attenuation coefficient with the increase in photon energy.

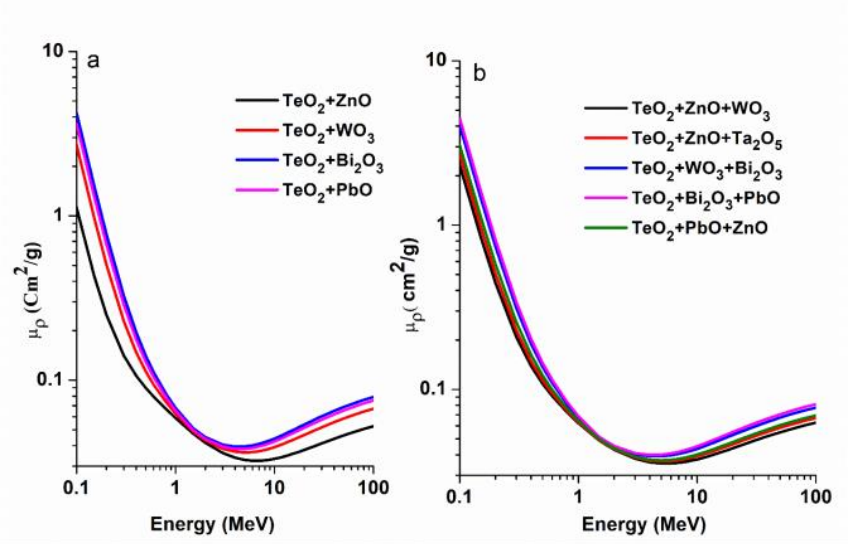

Figure 1: The study of the mass attenuation coefficient is presented in Figure 1. Figure 1(a) illustrates the dependence of the mass attenuation coefficient for each binary mixture with TeO_2, and Figure 1(b) illustrates the dependence for the ternary mixture with respect to TeO_2.

Figures 2a, 2c, and 2e represent the mass attenuation coefficient for the binary mixture in the energy spectrum between 100 and 600 keV with a remarkable trend. Among the binary systems, TeO_2 combined with Bi_2O_3 reflects the highest mass attenuation coefficient beyond all other combinations in the whole energy spectrum. That reflects that the TeO_2+Bi_2O_3 combination shows better photon attenuation properties than other binary systems. Consequently, TeO_2 + PbO shows a relatively high value of mass attenuation coefficient, which is, however, always lower than TeO_2 + Bi_2O_3. These results thus indicate that the incorporation of Bi_2O_3 significantly enhances the efficiency of photon attenuation in the material and thus increases its effectiveness in energy absorption in the concerned energy range.

In contrast, Figs. 2b, 2d, and 2f depict, in the same energy interval, the mass attenuation coefficients obtained for ternary combinations: The highest value of MAC for ternary systems provides TeO_2 + Bi_2O_3 + PbO, and thus this combination was most efficient in the attenuation of photons. TeO_2 + WO_3+ Bi_2O_3 also gives a remarkable mass attenuation coefficient, though it was slightly lower than in the case of TeO_2 + Bi_2O_3 + PbO system. The results obtained revealed that the addition of Bi_2O_3 enhances the capability of photon absorption of the ternary mixes, in particular when combined with PbO or WO_3, within the specified energy range.

Further research has demonstrated that the mass attenuation coefficient of a binary mixture of TeO_2 + Bi_2O_3 has diminished considerably with an increase in photon energy. For example, a decrease in the mass attenuation coefficient is observed by about 96.5% when the photon energies increase from 100 to 500 keV and by about 78% from 200 to 600 keV. This represents the ternary mixture of TeO_2, Bi_2O_3, and PbO with a significant drop to 96.87% at 100 and 500 keV and 81.67% at 200 and 600 keV. These results illustrate that mixes containing heavy metals like PbO and Bi_2O_3 have very good X-rays and gamma rays attenuation capability, especially at a special energy range, making them highly effective in radiation shielding applications.

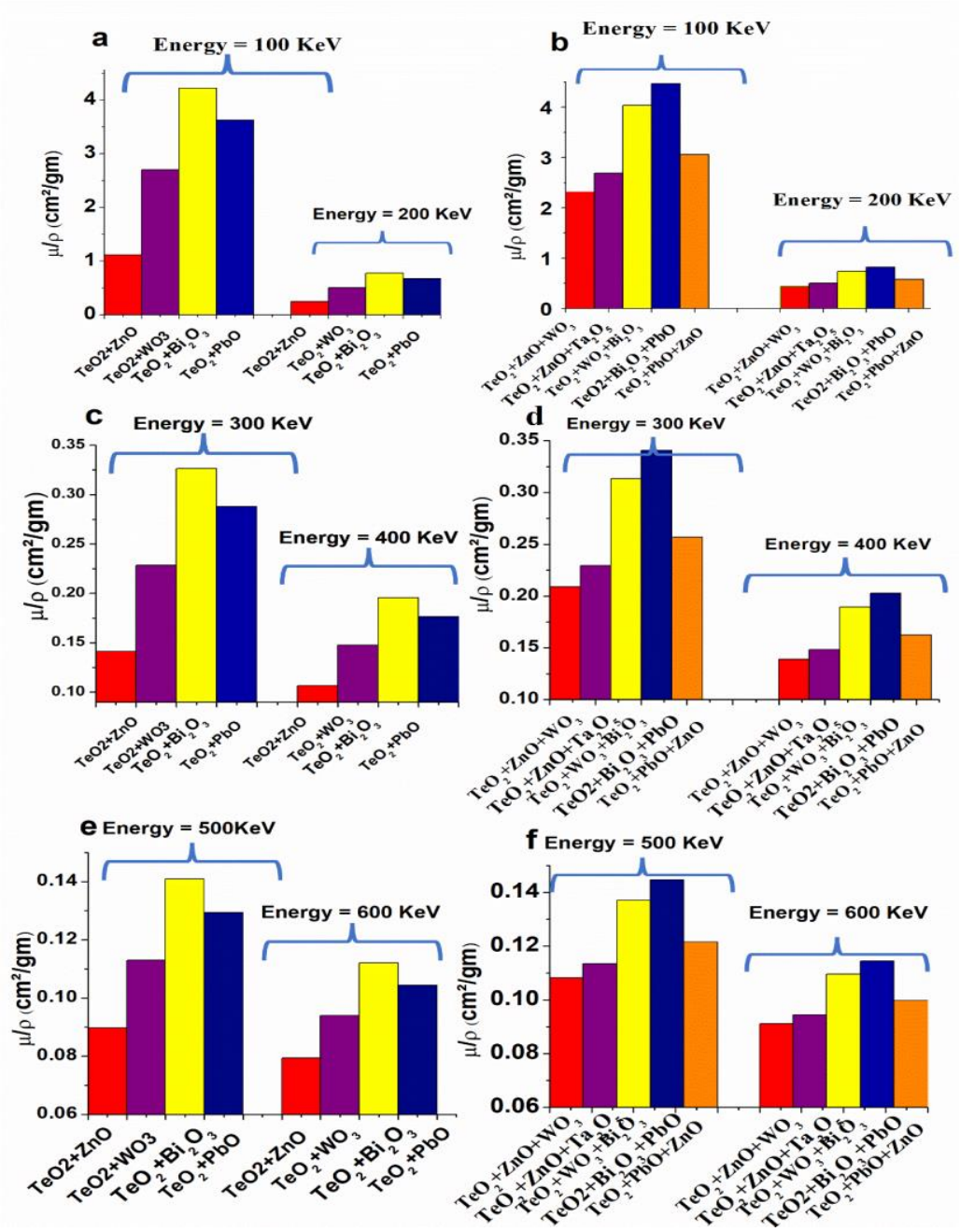

Figure 2: "The mass attenuation coefficient (μ/ρ) of some TeO_2-based binary and ternary mixture at different energies."

3.2 Effective atomic number (Z_{eff})

Z_{eff} is considered the atomic number average of every material or mixture that is normally used, given the elemental composition and type of radiation interaction of interest. The calculation of Z_{eff} for a shielding material will, therefore, help foresee its performance in radiation protection. Zeff is an important parameter to understand and thus optimize the performance of a material in high-energy photon shielding applications.

Fig. 3 reports that at 0.1 MeV, maximum Zeff has been determined to be around the binary mixtures of TeO_2 + $Bi_2O_3$with Z_{eff} = 75 and TeO_2+ PbO with Z_{eff} = 72. At the initial energy, the studied mixtures have a maximum increase in their values. Above 1.05 MeV minima was the obtained value for both the above mixtures42 Among the ternary mixtures of the glass system TeO_2 + ZnO + WO_3, TeO_2 +

$ZnO + Ta_2O_5$, $TeO_2 + WO_3 + Bi_2O_3$, $TeO_2 + Bi_2O_3 + PbO$, and $TeO_2 + PbO + ZnO$, the maximum values of Zeff have been recorded in the $TeO_2 + WO_3 + Bi_2O_3$ mixture at Z_{eff} of 74 and in the $TeO_2 + PbO + ZnO$ mixture at Z_{eff} of 68.5.

For the present ternary systems, minimum values of Z_{eff} are observed at 1.05 MeV energy level. Generally, the higher the value of an effective atomic number (Z_{eff}) better the shielding material for photons like X-rays and γ-rays.

A high Z_{eff} will mean that the material is more effective in attenuating the radiation and is thus the best choice for the application of radiation shielding. It gives the capability of a material to interact with and effectively stop the radiation.

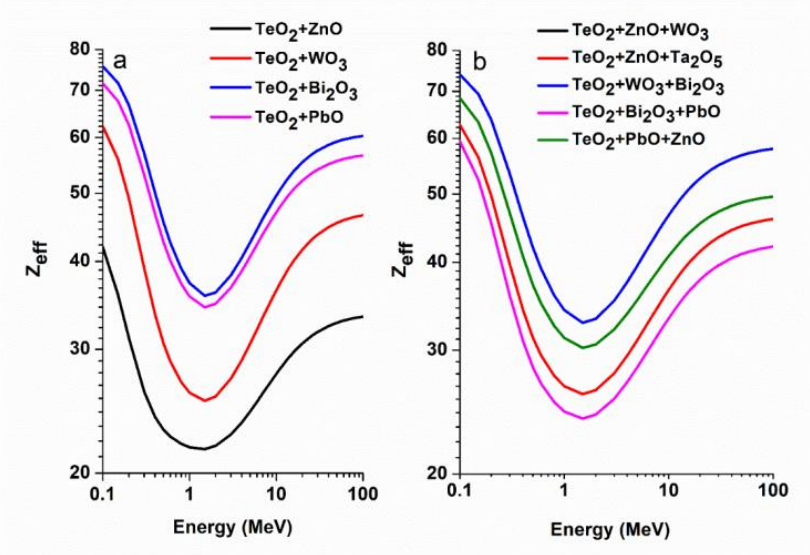

Figure 3: "Effective atomic number (Zeff) for some TeO_2-based binary and ternary mixtures at different energies."

3.3 Effective electron density (N_{eff}):

The effective electron density, Neff, is the total number of electrons in a substance per unit mass. [42] It is an important parameter in radiation shielding because it shows the number of electrons that can interact with the incoming radiation. This parameter is essential for understanding how different materials attenuate various forms of radiation, especially in X-ray and gamma-ray shielding.[43]

Further, we have computed the effective electron density, N_{eff}, for binary mixtures of $TeO_2 + ZnO$, $TeO_2 + WO_3$, $TeO_2 + Bi_2O_3$, and $TeO_2 + PbO$ in the glass network. N_{eff} is defined as the electron density per unit mass in the samples of glass. The results reflected that the N_{eff} of WO_3, Bi_2O_3 glass system at 0.1 MeV was at its maximum values as 6.65 x 10^{23} and 5.8 x 10^{23} electrons per gram, which was depicted in Figure 4.[28] We then measured (N_{eff}), defined as the number of electrons per unit mass of ternary mixtures $TeO_2 + ZnO + WO_3$, $TeO_2 + ZnO + Ta_2O_5$, $TeO_2 + WO_3 + Bi_2O_3$, $TeO_2 + Bi_2O_3 + PbO$, and $TeO_2 + PbO + ZnO$ in a glass system. The results obtained showed that in the TeO_2-based glasses with $ZnO + WO_3$ and $ZnO + Ta_2O_5$ additions, the maximum N_{eff} values were 6.75 x 10^{23} and 6.65 x 10^{23} electrons per gram at 0.1 MeV, respectively. It was concluded from this study that at low photon energy, the binary combinations in TeO_2, ZnO, WO_3, Bi_2O_3, and PbO showed a high value of N_{eff}, which is indicative of high electron concentration. With the rise in the energy of photons, N_{eff} decreased, which means the electron density has decreased. This trend has been consistent for all three ternary glass compositions tested, where N_{eff} was very low at 1.1 MeV, indicating low interaction of electrons with photons of higher energy. A higher (N_{eff}) is often advantageous for shielding

applications as it improves the material's capacity to absorb and attenuate radiation. Consequently, materials exhibiting elevated N_{eff} values are advantageous for the design of radiation shielding.

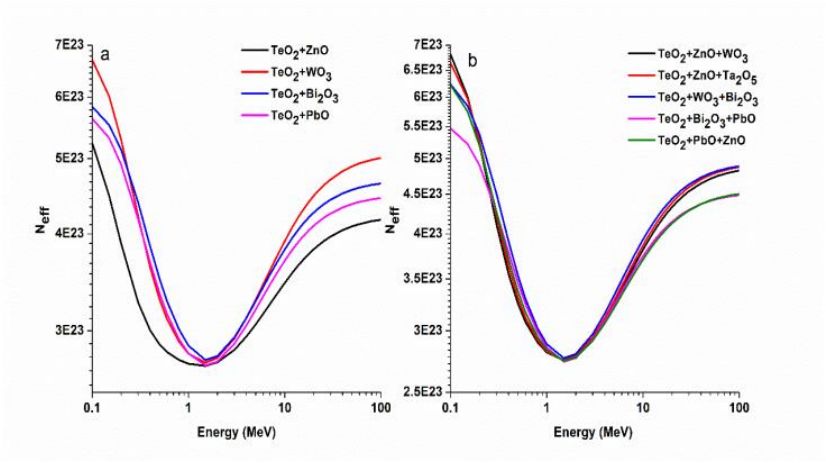

Figure 4: illustrates the effective electron density (N_{eff}) for several TeO_2-based binary and ternary combinations across different energy levels.

3.4 Half-value layer

The half-value layer (HVL), also referred to as half-value thickness, is defined as the thickness of a material required to reduce the intensity of incident radiation by 50%. While HVL and the mean free path (MFP) are interrelated, they describe distinct aspects of radiation interaction with materials. The MFP represents the average distance a radiation particle travels within a material before undergoing absorption or scattering, whereas the HVL quantifies the material thickness needed to attenuate half of the incoming radiation.[4,44-45]

In addition to HVL, three other widely used transmission factors for characterizing photon attenuation are the tenth-value layer (TVL), HVT, and MFP. Lower values for these transmission factors are indicative of more effective attenuation because they require less volume of material to absorb a certain amount of radiation.

The Phy-X/PSD program was employed in the present study to calculate such transmission factors for binary and ternary glass systems at various energy levels.

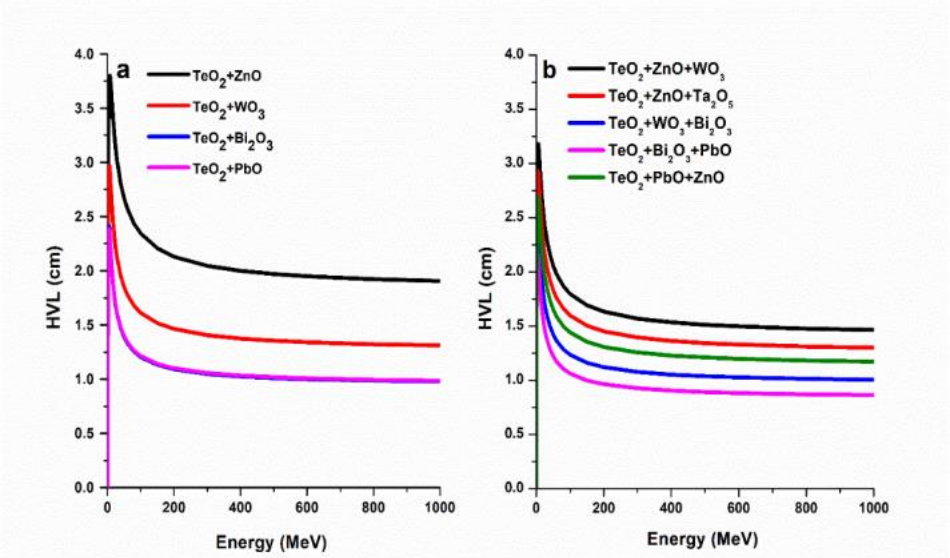

Figure 5: The half-value layer layers for different TeO_2-based binary and ternary mixtures between 0 MeV and 1000 MeV.

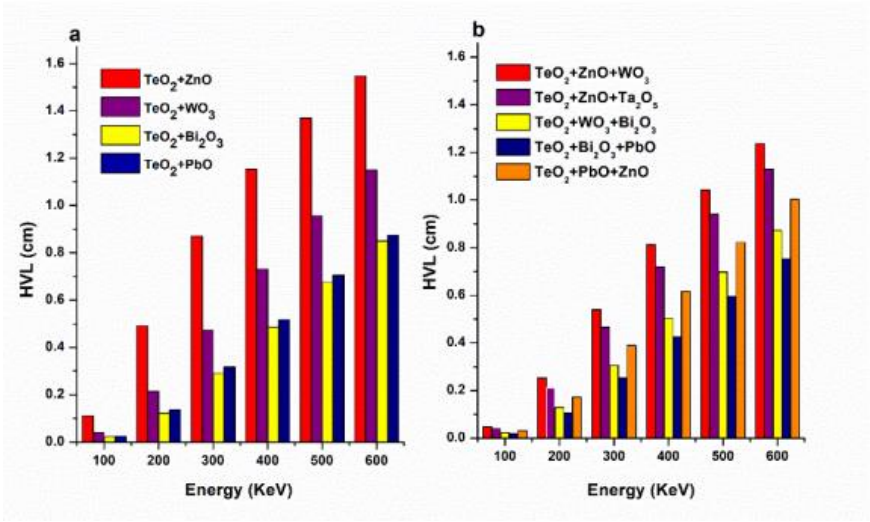

Figure 6: Half-value thickness for some binary and ternary mixtures of TeO2 in the energy range of 100-600 keV.

The HVL values for various binary and ternary glass mixtures, such as TeO_2 + ZnO, TeO_2 + WO_3, TeO_2 + Bi_2O_3, and TeO_2 + PbO, and ternary mixtures like TeO_2 + ZnO + WO_3, TeO_2 + ZnO + Ta_2O_5, TeO_2 + WO_3 + Bi_2O_3, TeO_2 + Bi_2O_3 + PbO, and TeO_2 + PbO + ZnO, were investigated in detail within the energy range of 0 MeV to 1000 MeV, as shown in Fig.5.

Notably, the binary mixtures TeO_2 + ZnO, TeO_2 + WO_3, and the ternary ones of TeO_2 + ZnO + WO_3 and TeO_2 + ZnO + Ta_2O_5 exhibit high HVL values and low mass attenuation coefficients. It means that high-energy particles can pass with small attenuation in these materials and become very suitable for those cases of applications where the minimal interaction of radiation is demanded, for example, particular optical or radiation-permissive devices.

The combinations of TeO_2 + Bi_2O_3, TeO_2 + PbO, TeO_2 + WO_3 + Bi_2O_3, and TeO_2 + Bi_2O_3 + PbO possess lower HVL and greater mass attenuation coefficient values; therefore, these glasses are better at attenuating radiation. The increase in the mass attenuation coefficient will provide more opportunities to decrease the shielding thickness of radiation protection devices using these glasses. The high HVL

values found in all glass samples show the excellent performance of the developed TeO_2-based glasses containing various metal oxides to effectively attenuate X-ray photons.

Fig.6 depicts the relationship between HVT and various energy compositions. The chart illustrates that HVT is inversely related to the linear attenuation coefficient (μ), as represented by the subsequent formula. (HVL=0.693/μ) As shown in Fig.6, glass systems containing TeO_2 + Bi_2O_3 and TeO_2 + Bi_2O_3 + PbO exhibited the lowest HVT values, indicating the best attenuation performance.

In contrast, the systems including TeO_2 + ZnO and TeO_2 + ZnO + WO_3 exhibited the least effective attenuation properties. Fig.6 illustrates that HVT escalates with increasing photon energy, indicating that thinner shielding materials are sufficient for low-energy photons, whereas bigger thicknesses are required for good protection against high-energy photons.

3.5 Tenth value layer

The tenth-value layer (TVL) is the average material thickness required to absorb 90% of incident radiation and reduce its intensity to one-tenth of the initial. A single TVL equals or is more than log2(10)log2(10), which is approximately 3.32 half-value layers (HVLs) with equality being valid for a monoenergetic beam of radiation. TVL values for various binary and ternary glass mixtures, including TeO_2 + ZnO, TeO_2 + WO_3, TeO_2 + Bi_2O_3, and TeO_2 + PbO, as well as ternary combinations such as TeO_2 + ZnO + WO_3, TeO_2 + ZnO + Ta_2O_5, TeO_2 + WO_3 + Bi_2O_3, TeO_2 + Bi_2O_3 + PbO, and TeO_2 + PbO + ZnO, have been extensively analyzed over an energy range of 0 MeV to 1000 MeV, as illustrated in Fig. 7.

Among these mixtures, the glass combinations TeO_2 + ZnO, TeO_2 + WO_3, and the ternary mixtures TeO_2 + ZnO + WO_3 and TeO_2 + ZnO + Ta_2O_5 are noted for their high TVL values and low mass attenuation coefficients. This suggests that these materials are effective in allowing high-energy particles to pass through with minimal attenuation, making them suitable for applications where reduced interaction with radiation is desired.

Fig.8 presents the computed tenth-value layer (TVL) for various binary and ternary glass systems at different energy levels. The investigated glass compositions encompass systems including TeO_2 + ZnO, TeO_2 + WO_3, TeO_2 + Bi_2O_3, TeO_2 + PbO, as well as combinations such as TeO_2 + ZnO + WO_3, TeO_2 + ZnO + Ta_2O_5, TeO_2 + WO_3 + Bi_2O_3, TeO_2 + Bi_2O_3 + PbO, and TeO_2 +PbO ZnO.

Fig. 8 demonstrates a fast escalation in the total volume loss (TVL) for all glass systems up to 0.6 MeV with increasing photon energy, succeeded by a more steady rise at elevated energy levels. This pattern underscores the energy dependency of photon attenuation, indicating that greater energies necessitate thicker material layers for adequate shielding. Forty-five
The TVL results indicate that the glasses comprising TeO_2 + Bi_2O_3 and TeO_2 + Bi_2O_3 + PbO had superior attenuation performance at all energy levels. The enhanced performance is ascribed to the decrease in TVL with elevated TeO_2 concentration, which augments the material's capacity to attenuate photons. Conversely, the systems including TeO_2 + ZnO and TeO_2 + ZnO + WO_3 demonstrated the least effective attenuation, as evidenced by their elevated TVL values in Fig. 6. The findings demonstrate that the TVL ratio among the samples was comparatively elevated at reduced photon energy. It also means that TeO_2 had a significant effect on the TVL by causing an improved shielding efficiency for lower energies compared with the higher energies. Further authentication on the TVL disclosed that samples containing high fractions of TeO_2, especially incorporating Bi_2O_3, and the combination Bi_2O_3 + PbO showed improved attenuation features; these are more adequate in medical applications such as computed tomography scan or diagnostic imaging, which may need frequent use of low-energy photons. Their suitability for these applications is due to the sufficiency of the shielding

against gamma radiation at these reduced energies. Fig. 7 The tenth value layers for the different TeO_2-based Binary and Ternary mixtures between 0 MeV and 1000 MeV.

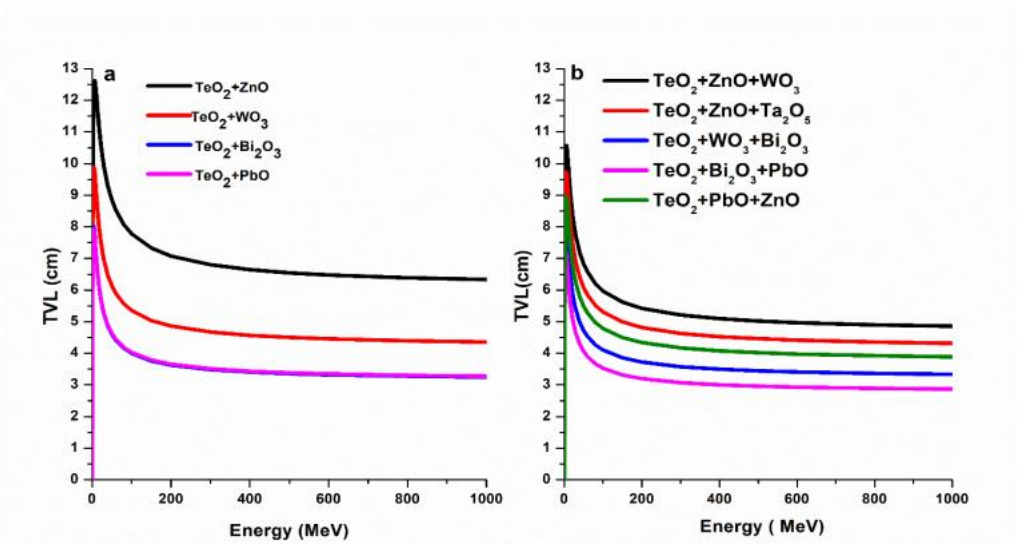

Figure 7: The tenth value layers for different TeO_2-based binary and ternary mixtures between 0 MeV and 1000 MeV.

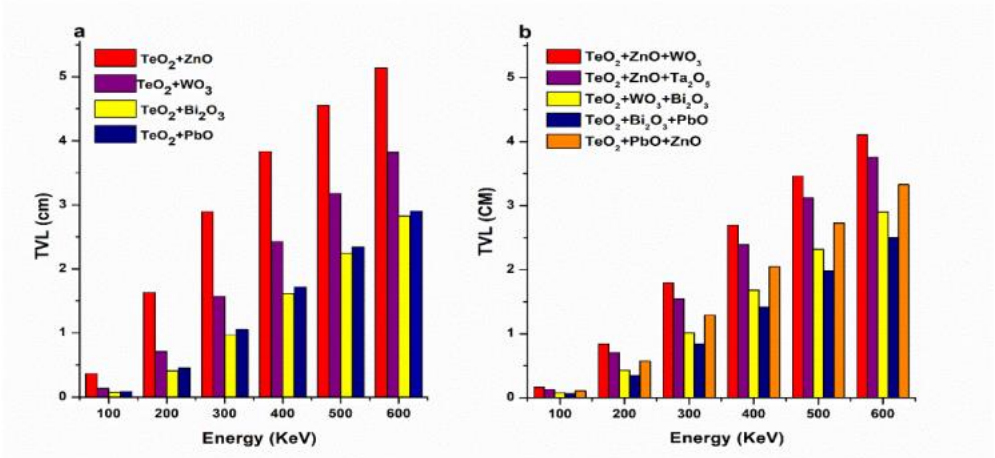

Figure 8: The tenth value layers for different TeO_2-based binary and ternary mixtures between 100 keV and 600 keV.

The rest of the mixtures-TeO_2 + Bi_2O_3, TeO_2 + PbO, TeO_2 + WO_3 + Bi_2O_3, and TeO_2 + Bi_2O_3 + PbO-have a lower value of TVL and a high mass attenuation coefficient. All these materials are more efficient in attenuating radiation; this is an indication of better suitability for applications that require immense radiation shielding.

3.6 Mean Free Path:

MFP is an essential concept in medical imaging, radiation therapy, nuclear medicine, and radiation safety, providing significant insight into the optimization of diagnostic procedures, treatment precision, and safety for both patients and medical personnel. In general, in radiation shielding, MFP refers to the average distance that particles, such as photons, neutrons, or charged particles, travel through a material before undergoing significant interactions like absorption or scattering. Knowledge of MFP is imperative in the design of appropriate shielding materials to block harmful radiation by reducing its intensity.[46]

MFP values for a range of binary and ternary glass mixtures, including TeO_2 + ZnO, TeO_2 + WO_3, TeO_2 + Bi_2O_3, and TeO_2 + PbO, as well as ternary combinations such as TeO_2 + ZnO + WO_3, TeO_2 + ZnO + Ta_2O_5, TeO_2 + WO_3 + Bi_2O_3, TeO_2 + Bi_2O_3 + PbO, and TeO_2 + PbO + ZnO, have been thoroughly investigated over an energy range of 0 MeV to 1000 MeV, as depicted in

Fig. 9. Indeed, this large energy window encompasses considerable variations in the incoming particles' energy and would, therefore, allow detailed evaluation of the MFP values for these various glass compositions and energies.

Notably, the three-component glasses among glass TeO_2 + ZnO, TeO_2 + WO_3, TeO_2 + ZnO + WO_3, and TeO_2 + ZnO Ta_2O_5 have presented high values of MFP while minimum mass attenuation coefficient.

That means the materials are very effective at allowing high-energy particles to pass through them with minimal interaction; hence, these materials find applications in areas where low radiation attenuation and high penetration power are required. The obtained data underlines the importance of these compositions in optimizing radiation shielding and other high-energy particle applications. The MFPs of various binary and ternary glass mixtures are represented graphically in Fig. 10. The binary mixtures of glass systems studied are TeO_2 + ZnO, TeO_2 + WO_3, TeO_2 + Bi_2O_3, and TeO_2 + PbO, while some ternary combinations include TeO_2 + ZnO + WO_3, TeO_2 + ZnO + Ta_2O_5, TeO_2 + WO_3 + Bi_2O_3, TeO_2 + Bi_2O_3 + PbO, and TeO_2 + PbO + ZnO. These mixtures were studied in an energy range from 100 keV to 600 keV, for MFP values from 0 to 2.5 cm.. The results presented an explicit trend: for every glass specimen, as the photon energy increases, the MFP also does, in a monotonic fashion. This increase is related to the behavior of μ, which decreases with the increase of energy, as will be shown in Fig. 2. Since the MFP is inversely proportional to the mass attenuation coefficient, this relationship explains the observed trend. [28]

The findings underscore the importance of material composition in determining the effectiveness of shielding, as higher MFP values indicate a lower ability of the material to attenuate radiation at higher energy levels."

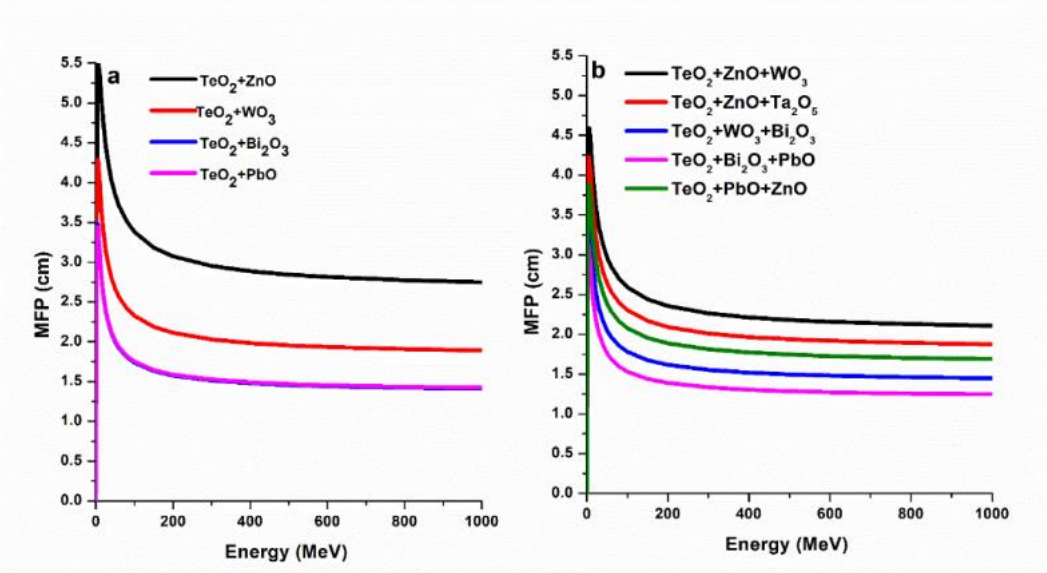

Figure 9: The Mean Free Path for different TeO_2-based binary and ternary mixtures between 0 MeV and 1000 MeV.

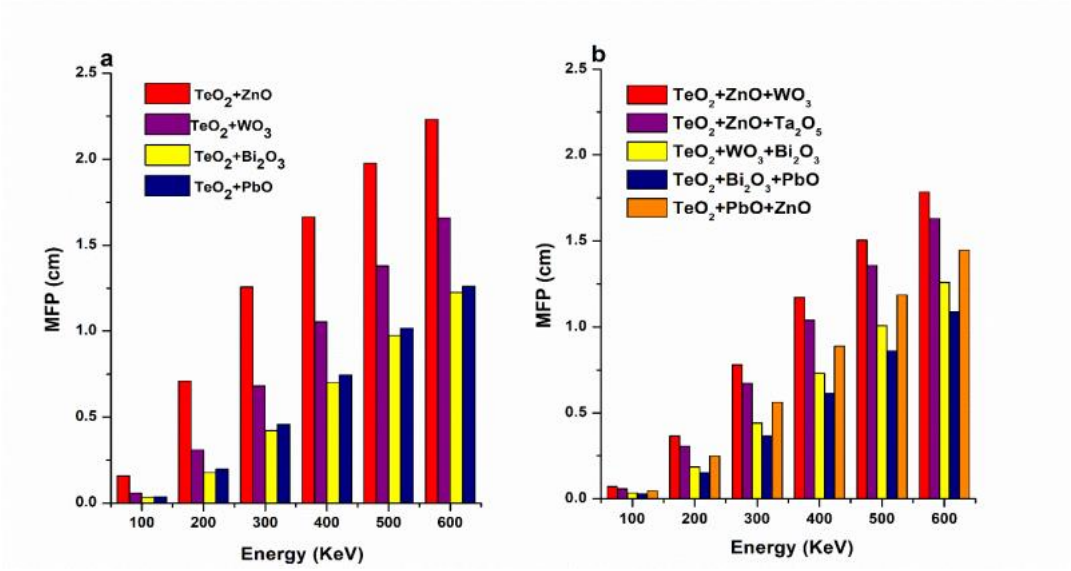

Figure 10: The Mean Free Path for different TeO_2-based binary and ternary mixtures between 100 keV and 600 keV.

4. Conclusion

The present article reports an extended theoretical analysis of radiation shielding characteristics in binary and ternary tellurite glasses. Based on the result obtained, the addition of heavy metals, especially Bi_2O_3 and PbO, effectively enhanced the shielding performance of TeO_2-based glass systems. The following are some important features emanating from the results of the analysis obtained:

1. mass attenuation coefficient (μ/ρ): TeO_2 + Bi_2O_3 and TeO_2 + PbO combinations are highly attractive for high photon attenuations, especially for low-energy photons. For the ternary systems, maximum attenuation was recorded in the TeO_2 + Bi_2O_3 + PbO due to complementary effects caused by heavy metal addictions.
2. Effective Atomic Number (Zeff): The highest values of Zeff are observed for the systems containing Bi_2O_3-PbO, which represents the great potential of these oxides for better interaction with photons. The TeO_2 + Bi_2O_3 + PbO ternary combination shows outstanding Zeff.
3. Effective Electron Density (Neff): High Neff values confirm an increase in the number of interactions between electrons with photons in TeO_2-based glasses containing heavy elements at low energies of photons.
4. Half-value Layer and Tenth-Value Layer: Minimum values of HVL and TVL are obtained in the case of TeO_2 + Bi_2O_3 and TeO_2+Bi_2O_3 + PbO systems, and these exhibit their highest efficiency as a shielding material. Higher values of the same have been found in the combinations containing ZnO and WO_3, which may be used at places where minimum interaction is required with the radiation.

The obtained results indicate that Bi_2O_3- and PbO-doped tellurite glasses are promising materials for radiation shielding applications due to their higher attenuation, high Zeff, and efficient electron density. These materials hold immense potential for advanced shielding applications in medical, industrial, and nuclear fields. Further experimental studies are suggested to confirm these theoretical predictions and explore their practical implementation.

Author's Contribution

We confirm that all named authors have read and approved the manuscript. We also confirm that each author has made a comparable contribution to the paper. We further confirm that all authors have approved the order of authors listed in the manuscript

Conflict of Interest

The authors declare no conflict of interest

Acknowledgment

Didar Swara Salih: Conceptualization, Investigation, Formal analysis, Shaida Anwer Kakil: Conceptualization, Visualization, Validation, Writing—review & editing, Resources and Supervision. Mohammed Issa Hussein: formal analysis, Validation, Writing, review, and editing.

Reference

[1] Bilir G. Synthesis and spectroscopy of Nd3+-doped tellurite-based glasses. *Int J Appl Glas Sci*. 2015;6(4):397-405. https://doi.org/10.1111/ijag.12124

[2] Bilir G, Yüksek M, Karatay A, Elmalı A. Nonlinear optical absorption properties of tellurium glasses containing different network modifiers. *J Opt*. 2020;22(7):75501. https://doi.org/10.1088/2040-8986/ab92b6

[3] Paz EC, Dias JDM, Melo GHA, et al. Physical, thermal and structural properties of Calcium Borotellurite glass system. *Mater Chem Phys*. 2016;178:133-138. https://doi.org/10.1016/j.matchemphys.2016.04.080

[4] Al-Hadeethi Y, Sayyed MI. Using Phy-X/PSD to investigate gamma photons in SeO2–Ag2O–TeO2 glass systems for shielding applications. *Ceram Int*. 2020;46(8):12416-12421. https://doi.org/10.1016/j.ceramint.2020.02.003

[5] Rammah YS, Kavaz E, Perişanoğlu U, Kilic G, El-Agawany FI, Tekin HO. Charged particles and gamma-ray shielding features of oxyfluoride semiconducting glasses: TeO2-Ta2O5-ZnO/ZnF2. *Ceram Int*. 2020;46(16):25035-25042. https://doi.org/10.1016/j.ceramint.2020.06.289

[6] Al-Hadeethi Y, Sayyed MI. Radiation attenuation properties of Bi2O3–Na2O–V2O5–TiO2–TeO2 glass system using Phy-X/PSD software. *Ceram Int*. 2020;46(4):4795-4800. https://doi.org/10.1016/j.ceramint.2019.10.212

[7] Kamalam EB, Manikandan N. Recent advances in bismuth tellurite glasses for photonic and radiation shielding applications. *ECS J Solid State Sci Technol*. 2023;12(7):76007. https://doi.org/10.1149/2162-8777/ace6d8

[8] Kirdsiri K, Kaewkhao J, Pokaipisit A, Chewpraditkul W, Limsuwan P. Gamma-rays shielding properties of xPbO:(100−x)B2O3 glasses system at 662keV. *Ann Nucl Energy*. 2009;36(9):1360-1365. https://doi.org/10.1016/j.anucene.2009.06.019

[9] Salehizadeh SA, Melo BMG, Freire FNA, Valente MA, Graça MPF. Structural and electrical properties of TeO2–V2O5–K2O glassy systems. *J Non Cryst Solids*. 2016;443:65-74. https://doi.org/10.1016/j.jnoncrysol.2016.03.012

[10] Elkhoshkhany N, El-Mallawany R, Syala E. Mechanical and thermal properties of TeO2–Bi2O3–V2O5–Na2O–TiO2 glass system. *Ceram Int*. 2016;42(16):19218-19224. https://doi.org/10.1016/j.ceramint.2016.09.086

[11] Sayyed MI, Elhouichet H. Variation of energy absorption and exposure buildup factors with incident photon energy and penetration depth for boro-tellurite (B2O3-TeO2) glasses. *Radiat Phys Chem*. 2017;130:335-342. https://doi.org/10.1016/j.radphyschem.2016.09.019

[12] Gaikwad DK, Obaid SS, Sayyed MI, et al. Comparative study of gamma ray shielding competence of WO3-TeO2-PbO glass system to different glasses and concretes. *Mater Chem Phys*. 2018;213:508-517. https://doi.org/10.1016/j.matchemphys.2018.04.019

[13] Ersundu AE, Büyükyıldız M, Ersundu MÇ, Şakar E, Kurudirek M. The heavy metal oxide glasses within the WO3-MoO3-TeO2 system to investigate the shielding properties of radiation applications. *Prog Nucl Energy*. 2018;104:280-287. https://doi.org/10.1016/j.pnucene.2017.10.008

[14] Al-Buriahi MS, Alrowaili ZA, Eke C, Alzahrani JS, Olarinoye IO, Sriwunkum C. Optical and radiation shielding studies on tellurite glass system containing ZnO and Na2O. *Optik (Stuttg)*. 2022;257:168821. https://doi.org/10.1016/j.ijleo.2022.168821

[15] de Clermont-Gallerande J, Saito S, Colas M, Thomas P, Hayakawa T. New understanding of TeO2–ZnO–Na2O ternary glass system. *J Alloys Compd*. 2021;854:157072. https://doi.org/10.1016/j.jallcom.2020.157072

[16] Halimah MK, Azuraida A, Ishak M, Hasnimulyati L. Influence of bismuth oxide on gamma radiation shielding properties of boro-tellurite glass. *J Non Cryst Solids*. 2019;512:140-147. https://doi.org/10.1016/j.jnoncrysol.2019.03.004

[17] El-Khayatt AM, Ali AM, Singh VP. Photon attenuation coefficients of Heavy-Metal Oxide glasses by MCNP code, XCOM program and experimental data: A comparison study. *Nucl Instruments Methods Phys Res Sect A Accel Spectrometers, Detect Assoc Equip*. 2014;735:207-212. https://doi.org/10.1016/j.nima.2013.09.027

[18] Dong MG, Agar O, Tekin HO, Kilicoglu O, Kaky KM, Sayyed MI. A comparative study on gamma photon shielding features of various germanate glass systems. *Compos Part B Eng*. 2019;165:636-647. https://doi.org/10.1016/j.compositesb.2019.02.022

[19] Gaikwad DK, Sayyed MI, Botewad SN, et al. Physical, structural, optical investigation and shielding featuresof tungsten bismuth tellurite based glasses. *J Non Cryst Solids*. 2019;503-504:158-168. https://doi.org/10.1016/j.jnoncrysol.2018.09.038

[20] Gerward L, Guilbert N, Bjørn Jensen K, Levring H. X-ray absorption in matter. Reengineering XCOM. *Radiat Phys Chem*. 2001;60(1):23-24. https://doi.org/10.1016/S0969-806X(00)00324-8

[21] Gerward L, Guilbert N, Jensen KB, Levring H. WinXCom—a program for calculating X-ray attenuation coefficients. *Radiat Phys Chem*. 2004;71(3):653-654. https://doi.org/10.1016/j.radphyschem.2004.04.040

[22] Tuncel N, Akkurt I, Atik I, Boodaghi Malidarre R, Sayyed MI. Neutron-gamma shielding properties of chalcogenide glasses. *Radiat Phys Chem*. 2024;218:111582. https://doi.org/10.1016/j.radphyschem.2024.111582

[23] Akkurt I, Malidarre RB, Kavas T. Monte Carlo simulation of radiation shielding properties of the glass system containing Bi2O3. *Eur Phys J Plus*. 2021;136(3):1-10. https://doi.org/10.1140/epjp/s13360-021-01260-y

[24] El-bashir BO, Sayyed MI, Zaid MHM, Matori KA. Comprehensive study on physical, elastic and shielding properties of ternary BaO-Bi2O3-P2O5 glasses as a potent radiation shielding material. *J Non Cryst Solids*. 2017;468:92-99. https://doi.org/10.1016/j.jnoncrysol.2017.04.031

[25] Rammah YS, Olarinoye IO, El-Agawany FI, Mahmoud KA, Akkurt I, Yousef E. Evaluation of radiation shielding capacity of vanadium–tellurite–antimonite semiconducting glasses. *Opt Mater (Amst)*. 2021;114:110897. https://doi.org/10.1016/j.optmat.2021.110897

[26] Tekin HO, Abouhaswa AS, Kilicoglu O, Issa SAM, Akkurt I, Rammah YS. Fabrication, physical characteristic, and gamma-photon attenuation parameters of newly developed molybdenum reinforced bismuth borate glasses. *Phys Scr*. 2020;95(11):115703. https://doi.org/10.1088/1402-4896/abbf6e

[27] Hordieiev YS, Zaichuk A V. Study of the influence of R2O3 (R= Al, La, Y) on the structure, thermal and some physical properties of magnesium borosilicate glasses. *J Inorg Organomet Polym Mater*. 2023;33(2):591-598. https://doi.org/10.1007/s10904-022-02526-3

[28] Bashter II. Calculation of radiation attenuation coefficients for shielding concretes. *Ann Nucl Energy*. 1997;24(17):1389-1401. https://doi.org/10.1016/S0306-4549(97)00003-0

[29] Akkurt I, Akyildirim H, Mavi B, Kilincarslan S, Basyigit C. Gamma-ray shielding properties of concrete including barite at different energies. *Prog Nucl Energy*. 2010;52(7):620-623. https://doi.org/10.1016/j.pnucene.2010.04.006

[30] Akkurt I, Boodaghi Malidarreh P, Boodaghi Malidarre R. Simulation and prediction of the attenuation behaviour of the KNN–LMN–based lead-free ceramics by FLUKA code and artificial neural network (ANN)–based algorithm. *Environ Technol*. 2023;44(11):1592-1599. https://doi.org/10.1080/09593330.2021.2008017

[31] Akkurt I, Boodaghi Malidarre R. Gamma photon-neutron attenuation parameters of marble concrete by MCNPX code. *Radiat Eff Defects Solids*. 2021;176(9-10):906-918. https://doi.org/10.1080/10420150.2021.1975708

[32] Iskender Akkurt. Effective Atomic Numbers for Fe–Mn Alloy Using Transmission Experiment. *Chinese Phys Lett*. 2007;24(10):2812. https://doi.org/10.1088/0256-307X/24/10/027

[33] Akkurt I, El-Khayatt AM. The effect of barite proportion on neutron and gamma-ray shielding. *Ann Nucl Energy*. 2013;51:5-9. https://doi.org/10.1016/j.anucene.2012.08.026

[34] Akkurt I, Alomari A, Imamoglu MY, Ekmekçi I. Medical radiation shielding in terms of effective atomic numbers and electron densities of some glasses. *Radiat Phys Chem*. 2023;206:110767. https://doi.org/10.1016/j.radphyschem.2023.110767

[35] Gunoglu K, Varol Özkavak H, Akkurt İ. Evaluation of gamma ray attenuation properties of boron carbide (B4C) doped AISI 316 stainless steel: Experimental, XCOM and Phy-X/PSD database software. *Mater Today Commun*. 2021;29:102793. https://doi.org/10.1016/j.mtcomm.2021.102793

[36] Gunoglu K, Akkurt İ. Radiation shielding properties of concrete containing magnetite. *Prog Nucl Energy*. 2021;137:103776. https://doi.org/10.1016/j.pnucene.2021.103776

[37] Malidarre RB, Ozan Tekin H, Gunoglu K, Akyıldırım H. Assessment of Gamma Ray Shielding Properties for Skin. *Int J Comput Exp Sci Eng*. 2023;9(1):6-10. https://doi.org/10.22399/ijcesen.1247867

[38] Reda AM, El-Daly AA. Gamma ray shielding characteristics of Sn-20Bi and Sn-20Bi-0.4Cu lead-free alloys. *Prog Nucl Energy*. 2020;123:103304. https://doi.org/10.1016/j.pnucene.2020.103304

[39] Almuqrin AH, Sayyed MI. Radiation shielding characterizations and investigation of TeO 2–WO 3–Bi 2 O 3 and TeO 2–WO 3–PbO glasses. *Appl Phys A*. 2021;127:1-11. https://doi.org/10.1007/s00339-021-04344-9

[40] Dong M, Xue X, Kumar A, et al. A novel method of utilization of hot dip galvanizing slag using the heat waste from itself for protection from radiation. *J Hazard Mater*. 2018;344:602-614. https://doi.org/10.1016/j.jhazmat.2017.10.066

[41] Yasmin S, Rozaila ZS, Khandaker MU, et al. The radiation shielding offered by the commercial glass installed in Bangladeshi dwellings. *Radiat Eff defects solids*. 2018;173(7-8):657-672. https://doi.org/10.1080/10420150.2018.1493481

[42] Alkallas FH, Ben Gouider Trabelsi A, Elaissi S, et al. Investigation of the gamma photon shielding in Se–Te–Ag chalcogenide glasses using the Phy-X/PSD software. *Cogent Eng*. 2022;9(1):2116829. https://doi.org/10.1080/23311916.2022.2116829

[43] Chang Q, Guo S, Zhang X. Radiation shielding polymer composites: Ray-interaction mechanism, structural design, manufacture and biomedical applications. *Mater Des*. 2023;233:112253. https://doi.org/10.1016/j.matdes.2023.112253

[44] Waly ESA, Al-Qous GS, Bourham MA. Shielding properties of glasses with different heavy elements additives for radiation shielding in the energy range 15–300 keV. *Radiat Phys Chem*. 2018;150:120-124. https://doi.org/10.1016/j.radphyschem.2018.04.029

[45] Waly ESA, Fusco MA, Bourham MA. Gamma-ray mass attenuation coefficient and half value layer factor of some oxide glass shielding materials. *Ann Nucl Energy*. 2016;96:26-30. https://doi.org/10.1016/j.anucene.2016.05.028

[46] Kaur P, Singh KJ, Thakur S, Singh P, Bajwa BS. Investigation of bismuth borate glass system modified with barium for structural and gamma-ray shielding properties. *Spectrochim Acta Part A Mol Biomol Spectrosc*. 2019;206:367-377. https://doi.org/10.1016/j.saa.2018.08.038